SERBIAN JOURNAL OF ELECTRICAL ENGINEERING
Vol. 18, No. 3, October 2021, 351-384

UDC: 510.644.4:621.383.51]:004.94 **DOI: https://doi.org/10.2298/SJEE2103351B**

Fuzzy Logic Controller Based Maximum Power Point Tracking and its Optimal Tuning in Photovoltaic Systems

Noureddine Bouarroudj[1], Thameur Abdelkrim[1], Maissa Farhat[2], Vicente Feliu-Batlle[3], Boualam Benlahbib[1], Djamel Boukhetala[4], Fares Boudjema[4]

Abstract: Conventionally, the parameters of a fuzzy logic controller (FLC) are obtained by a trial and error method or by human experience. In this paper, the problem of designing a FLC for maximum power point tracking (MPPT) of a photovoltaic system (PV) that consists of a PV generator, a DC-DC boost converter and a lead-acid battery is studied. The normalization gains, the membership functions and the fuzzy rules are automatically adjusted using a particles swarm optimization algorithm (PSO) in order to maximize the criterion based on the integration of the PV module power under standard temperature condition (STC) (T=25ºC and S=1000 W/m^2). The robustness test of the optimized fuzzy logic MPPT controller (FLC-MPPT) is carried out under different scenarios. Simulation results of the system clearly show that the proposed optimized FLC-MPPT controller outperforms in terms of maximum efficiency the FLC-MPPT controller not optimized, the FLC-MPPT controller with optimized normalization gains and the FLC-MPPT controller with optimized normalization gains and membership functions.

Keywords: PV system, Boost converter, MPPT, FLC, FLC-MPPT, PSO, FLC-MPPT-PSO.

1 Introduction

Maximum power point tracking (MPPT) is one of the most important topics in power systems, especially in wind turbines and photovoltaic systems. In PV

[1]Unité de Recherche Appliquée en Energies Renouvelables, URAER, Centre de Développement des Energies Renouvelables, CDER, 47133, Ghardaïa, Algeria; E-mails: autonour@gmail.com; tameur3@gmail.com; bouallam30@gmail.com
[2]Department of Electrical, Electronics and Communications Engineering, American University of Ras Al Khaimah, Ras al-Khaimah, UAE; E-mail: maissa.farhat@gmail.com
[3]Escuela Técnica Superior de Ingenieros Industriales and Instituto de Investigaciones Energéticas y Aplicaciones Industriales, University of Castilla-La Mancha, Av. Camilo Jose Cela, S/N, C.P. 13001 Ciudad Real, Spain; E-mail: vicente.feliu@uclm.es
[4]Laboratoire de Commande des Processus, Ecole Nationale Polytechnique, 10 Rue des Frères OUDEK, El-Harrach 16200, Alger, Algeria; E-mails: djamel.boukhetala@g.enp.edu.dz; fboudjema@yahoo.fr

systems, several approaches have been proposed to overcome problems such as the undesirable oscillations around the maximum power point (MPP), non-robustness against load and weather conditions variations, which are present in methods like the classical perturb and observe (P&O) [1 – 3], Hill climbing [4, 5] and incremental conductance (INC) [6]. Fuzzy logic controllers that can be used for PV applications include the one of Mamdani and Takagi-Sugeno. The latter, which is one of the intelligent approaches, has become popular in the last two decades because of its large number of applications [7]. This approach does not require knowledge of the system's mathematical model, and provides better performance under variable climatic conditions. Depending on its inputs, which define the distance between the PV operating point and the MPP, this control system varies the output, which can minimize the oscillations around the MPP.

1.1 Hybridization of classical techniques with fuzzy logic

In [8 – 10], a FLC was used to generate a variable step size for the duty cycle of the DC-DC converter, resulting in reduced oscillations around the MPP. In [11], the authors used an FLC to generate a variable voltage step size for the optimal voltage generation in the classical P&O method, jointly with a proportional integral controller (PI) to generate the duty cycle that controls the DC-DC converter. This alleviates the oscillations around the MPP. A combination between P&O algorithm and FLC can also be found in [12], in which the P&O algorithm was used to generate the optimal PV module voltage whereas the FLC was used to generate the duty cycle in order to keep the PV module voltage (v_{pv}) at the optimal voltage ($v_{pv\text{-}opt}$). In [13], a two-stage MPPT controller strategy was employed. The first stage was used to generate the maximum power as the operating point and the second stage, which consists of a two-stage FLC, kept the PV system operating at MPP, and used the maximum power operating error and the ratio of the power change to produce the current change.

1.2 Direct fuzzy logic based MPPT controllers

An FLC-MPPT controller based on the slope $\tan(\theta_M) = i_{pv}/v_{pv} = 1$ was designed in [14]. The inputs of this controller are the difference between θ_M (the slope of the PV maximum power) and θ_C (the slope of the PV operating point), and the change of error. The output is the change in duty cycle. From simulation results, it can be seen that the FLC-MPPT was superior to the PI-MPPT controller. In this paper, θ_M was fixed at 45° and only temperature variation was considered. However, results can change if irradiance and temperature change simultaneously, because θ_M also would vary.

An FLC-MPPT was proposed in [15], which receives temperature and irradiance as its inputs; and its output is the estimated duty cycle corresponding to the MPP. Simulation and experimental results of this approach show its superior performance over the neural network and classical MPPT approaches.

The FLC-MPPT controllers designed in [16 – 33], have two inputs: the error (E) and the change of error, $\Delta E = E(k) - E(k-1)$, and one output which is the change of duty cycle, dα. An error $E = \Delta p_{pv}/\Delta v_{pv}$ was chosen in [16 – 29, 34], while an error $E = \Delta p_{pv}/\Delta i_{pv}$ was chosen in [30 – 33, 35]. The error E was used to determine the location of the system operating point: if it is on the right or the left half plane of the power-voltage curve of the PV module. On the other hand, the change of error was used to determine the magnitude of the duty cycle change to be added/subtracted to the duty cycle. In [36], ΔE was replaced by the change of voltage Δv_{pv}. This proposition can inform about the movement direction of the operating point. For example, when moving from the left to the right half plane of the $p_{pv} - v_{pv}$ curve, Δv_{pv} will increase, and vice versa. To address the variation of irradiance (fast or slow), authors in [37] have replaced the change in error (ΔE) by the change of power divided on power $\Delta p_{pv}/p_{pv}$, where $\Delta p_{pv}/p_{pv} > 0.01$ was considered a fast change of irradiance and $\Delta p_{pv}/p_{pv} < 0.01$ a slow change. According to this information, the change of duty cycle dα was calculated. In [38], the two input variables were selected as the derivative of power with respect to time $\mathrm{d}p_{pv}/\mathrm{d}t$ and the derivative of voltage with respect to time $\mathrm{d}v_{pv}/\mathrm{d}t$. If the MPP were achieved, these input variables would become equal to zero.

FLC-MPPT controllers proposed in [39 – 46] have the change of PV module power Δp_{pv} as their first input and the change of PV module voltage Δv_{pv}, or PV module current Δi_{pv}, as their second input. The output is always the duty cycle. These approaches are based on the classical P&O and hill climbing methods. The improvements in terms of settling time, accurate convergence and reduction of the oscillation were achieved by fuzzifying the rules of these methods. In [47], the authors have used Δv_{pv} nand Δi_{pv} as inputs.

In [48] a new FLC-MPPT controller has been proposed based on the classical flow chart of the optimal PV module current generator ($i_{pv\text{-}opt}$), in which the inputs were selected as $E = \Delta p_{pv} \cdot \Delta i_{pv}$ and $\Delta E = E(k) - E(k-1)$. Moreover, an adaptive gain was used in order to limit the variation of $i_{pv\text{-}opt}$.

In a PV system, when the maximum power is attained, the differentiation of the PV module power with respect to the PV module voltage ($\partial p_{pv}/\partial v_{pv}$) tends to zero, and then $v_{pv} \cdot (\partial i_{pv}/\partial v_{pv}) = -i_{pv}$. Based on these concepts, an FLC-MPPT with $E(k) = \mathrm{abs}(v_{pv}(k) \cdot (\Delta i_{pv}(k)/\Delta v_{pv}(k)))$ and $\Delta E(k)$ as inputs has been proposed in [49], designed in such a way that keep $E(k)$ in $i_{pv}(k)$.

To give more importance to the small variations of the PV module power and the PV module voltage, authors in [50] have designed a fractional order FLC-MPPT controller, in which the integer order derivative $E = \mathrm{d}p_{pv}/\mathrm{d}v_{pv}$ becomes of fractional order. In this case, $E = (\mathrm{d}^{\gamma} p_{pv})/(\mathrm{d}v_{pv}^{\gamma})$, where γ is a real number between 0 and 1, and the fractional order derivative can be computed using the Grunwald–Letnikov (GL) definition. Simulation and experimental results have shown the superiority of the fractional order FLC-MPPT over the integer order one in terms of transient and steady state performances.

As is known by the researchers in this field, the problem of partial shadow in a PV, where many MPP are created in the $p_{pv} - v_{pv}$ curve, can render the conventional FLC MPPT controller unable to track the global MPP. To tackle this problem, the authors in [51] designed an FLC-MPPT controller with a third input: the difference between the stored MPP (pm) and the actual power ($\Delta p_M = p_m(k) - p_{pv}(k)$). Also, to overcome the problem of the global MPP tracking, a fuzzy logic combined with a hill climbing was proposed in [52], in which the inputs of the FLC are the error $E = \Delta p_{pv}/\Delta v_{pv}$ and the change of power Δp_{pv}. In addition, an FLC-MPPT controller with compressed rules was proposed in [53]. This method used the change of power Δp_{pv}, the change of voltage Δv_{pv}, and the change in duty cycle $\Delta\alpha$ as inputs, the output being the reference current to the DC-DC converter. For making a decision about the MPPT condition, three rule lists were developed by combining the two input variables, and one new rule list was created among these three rules with the antecedent input parameters. The efficiency obtained by applying this strategy was about 99.5%. In order to simplify the number of fuzzy rules and cover larger operating conditions, a parameter β was added as a third input besides the change of power and the terminal voltage [54].

The real-time implementation of FLC-MPPT controller with two inputs is still complex and needs high-cost microcontrollers. Additionally, the number of membership functions and fuzzy rules has to be reduced. In this respect, single input FLC-MPPT controllers were proposed in [55 – 59]. Also, in order to solve the problem of the large computation time and the complexity of implementation, the FLC-MPPT controller was modelled using the M5P model tree, in which the FLC-MPPT controller was translated into a simple if-then instruction [60].

1.3 Determination of the FLC-MPPT parameters

The nonlinearity of the PV-systems, fast changes in weather conditions and load, and parameters tuning such as: the selection of membership functions (form and spacing), the normalization gains, and the fuzzy rules makes the designing of the FLC-MPPT controller very difficult. For these reasons, authors in [61] developed an asymmetrical FLC-MPPT controller in which triangular membership functions were used to reduce the computation complexity, and the universes of discourse of inputs and output variables were determined according to their variation range. Compared with conventional symmetrical FLC-MPPT controllers, the transient time and the MPPT precision were enhanced respectively by 42% and 0.06%.

In conventional FLC-MPPT controllers, the output dα is multiplied by a constant factor and, in order to reach rapidly the MPP without fluctuations, this constant factor is calculated by another FLC (see [62] for more details). The fuzzy rules of the second FLC are generated according to the distance between the PV module operating point and the MPP.

The difficulties of designing FLC-MPPT controllers have led some researchers (see [63, 64]) to move towards evolutionary algorithms because of their global exploration characteristics in a complex environment. The Ant Colony (AC) and the particle swarm (PSO) optimization algorithms have been used to tune the normalization gains (or scaling factors). Authors in [65 – 67] have designed FLC-MPPT controllers based on Genetic Algorithms (GA), where the GA was used to determine the optimal shape and spacing of the triangular membership functions along a fixed and symmetrical universe of discourse. The same procedure to design optimal FLC-MPPT controllers was followed using Hopfield Neural Networks [68], PSO algorithms [69, 70], and adaptive neuro-fuzzy inference Systems (ANFIS) [71]. In [72], PSO algorithms were utilized to tune the membership functions of an asymmetrical FLC, and simulation results showed the superiority of this optimized controller over the symmetrical one. In [73, 74], the universes of discourse of each variable was fixed between -1 and 1, and normalized using normalization gains. In these works, the membership functions and the gains were optimized using a PSO and GA algorithm. The tuning of membership functions and rules has been discussed in [75, 76]. In [75], fuzzy cognitive networks were used to tune the membership functions and rules. In [76], an adaptive method based on the fuzzy knowledge base and a learning mechanism was employed to optimize the peak of triangular membership functions and rules.

1.4 Contribution and paper organization

Independent optimization of the scaling factors, membership functions and fuzzy rules has not been carried out because the three parts cannot be dissociated. To obtain the best results, the vector of the parameters to be optimized should therefore contain these three parts: the scaling factors, membership functions and fuzzy rules. It is within this framework that our motivation and interest lie in the design of FLC-MPPT controllers by using PSO algorithms. The optimization process is done under the standard climatic condition ($T = 25$ºC and $S = 1000$ W/m^2), while the robustness test is performed under different profiles of climatic condition. The rest of this paper is organized as follows: In Section 2, a brief description is given of the PV module, its mathematical model and its electrical characteristics, as well as the type and description of the used DC-DC converter and the lead-acid battery used as load. In Section 3, a full detail about the MPPT controller based on fuzzy logic is given. Section 4 gives a review of the PSO algorithms, including their principle and mathematical model. The optimization of the FLC-MPPT controller, including normalization gains, membership functions and fuzzy rules is described in Section 5. Finally, simulation results and conclusions are provided in Sections 6 and 7, respectively.

2 PV System Description

The main scheme of the usual photovoltaic conversion chains, Fig. 1 is made up of: 1) a photovoltaic generator (PVG) (PV module or PV panel consisting of many PV modules), 2) a DC-DC converter used as an intermediary between the PVG and a DC load, 3) a MPPT controller that drives the DC-DC converter to track the maximum power point delivered by the PVG.

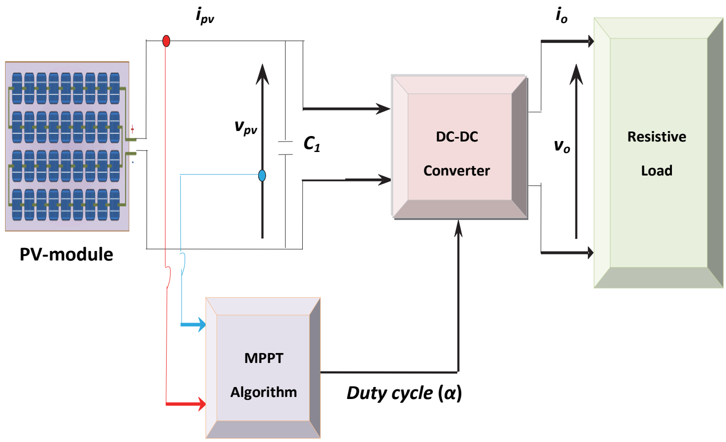

Fig. 1 – *Scheme of a PV system with a MPPT controller.*

The following subsections give details of each element.

2.1 PV module model and its characteristics

First of all, it is worth mentioning that the PV module is made up of PV cells, which are also made of different technologies, such as, crystalline silicon, thin film, and multijunction cells [77]. The latter are generally modelled by an electrical circuit (the single-diode model) [78, 79]. In spite of its simplicity, this model exhibits acute deficiencies when subject to temperature deviations. Moreover, its precision declines at low irradiance, particularly in the vicinity of the open circuit voltage (v_{oc}). So the two-diode model given by Fig. 2 is recommended for better accuracy [78 – 83].

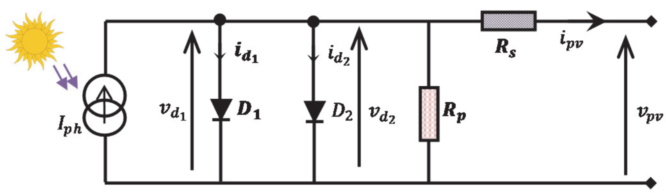

Fig. 2 – *Electrical circuit of a two-diode model of a photovoltaic cell.*

As shown in Fig. 2, a photovoltaic cell has a series resistor R_s and a shunt resistor R_p, which represent the power losses and the influence on the photovoltaic characteristic $i_{pv} - v_{pv}$. According to this figure, the mathematical model for the current-voltage characteristic of the PV module is given by [78, 80]:

$$\begin{aligned} N_p i_{pv} = i_{ph} - i_{s_1}\left(\exp\left(\frac{q(v_{pv}+i_{pv}N_sR_s)}{N_s n_1 kT}\right)-1\right)- \\ -i_{s_2}\left(\exp\left(\frac{q(v_{pv}+i_{pv}N_sR_s)}{N_s n_2 kT}\right)-1\right)-\frac{v_{pv}+i_{pv}N_sR_s}{N_sR_p}, \end{aligned} \tag{1}$$

where:

– i_{pv} and v_{pv} are the output current and voltage of the photovoltaic cell;

– i_{ph} is the produced photo-current ($S \cdot i_{ph\text{-max}}$), where S is the irradiance;

– i_{s1} and i_{s2} are the saturation currents of the diodes;

– n_1 and n_2 are the ideality factors of the diodes;

– N_s is the number of cells connected in series;

– N_p is the number of cells connected in parallel;

– k is the constant of Boltzmann (1.3806503×10^{-23} J/K);

– T is the temperature;

– q is the charge of electron (1.60217646×10^{-19} C).

Remark 1. To validate the PV module model, its parameters are usually identified or estimated in such a way to minimize a well-defined cost function in which the characteristics of the PV module model are close to the real characteristics of the PV module given in the datasheet [84 – 86].

Equation (1) shows that the current-voltage characteristic strongly depends on irradiance and temperature. The dependence on temperature is further amplified by the properties of the photo-current and the reverse saturation currents of the diodes, which are given by:

$$i_{ph}(T) = \frac{i_{ph-max}}{S_{stc}} S[1+(T-298)(5\cdot10^{-4})], \tag{2}$$

$$i_{s1} = K_1 T^3 \,\mathrm{e}^{\frac{-E_g}{kT}}, \tag{3}$$

$$i_{s2} = K_2 T^{\frac{5}{2}} \,\mathrm{e}^{\frac{-E_g}{kT}}, \tag{4}$$

where $E_g = -1.76\cdot10^{-19}$ represents the Band-Gap energy of the semiconductor, S_{stc} is the irradiance at the standard temperature condition (1000 W/m^2), and:

$$K_1 = 1.2 \text{ A/cm}^2\text{K}^3,$$
$$K_2 = 2.9 \cdot 10^5 \text{ A/cm}^2\text{K}^{5/2}. \tag{5}$$

Table 1 shows the specifications of this module. Figs. 3a and 3b show the p_{pv} (v_{pv}) and i_{pv} (v_{pv}) curves as a function of irradiance and temperature changes, respectively.

Table 1
Specifications used for the PV module [80].

Maximum Power $P_{\max}$	61.91 W
Open Circuit Voltage v_{oc}	25.25 V
Short Circuit Current $i_{ph\text{-max}}$	3.25 A
Voltage at Maximum Power v_{opt}	20 V
Current at Maximum Power i_{opt}	≈3.1 A
Ideality factor n_1	1
Ideality factor n_2	2
Number of series cells N_s	36
Number of parallel cells N_p	14

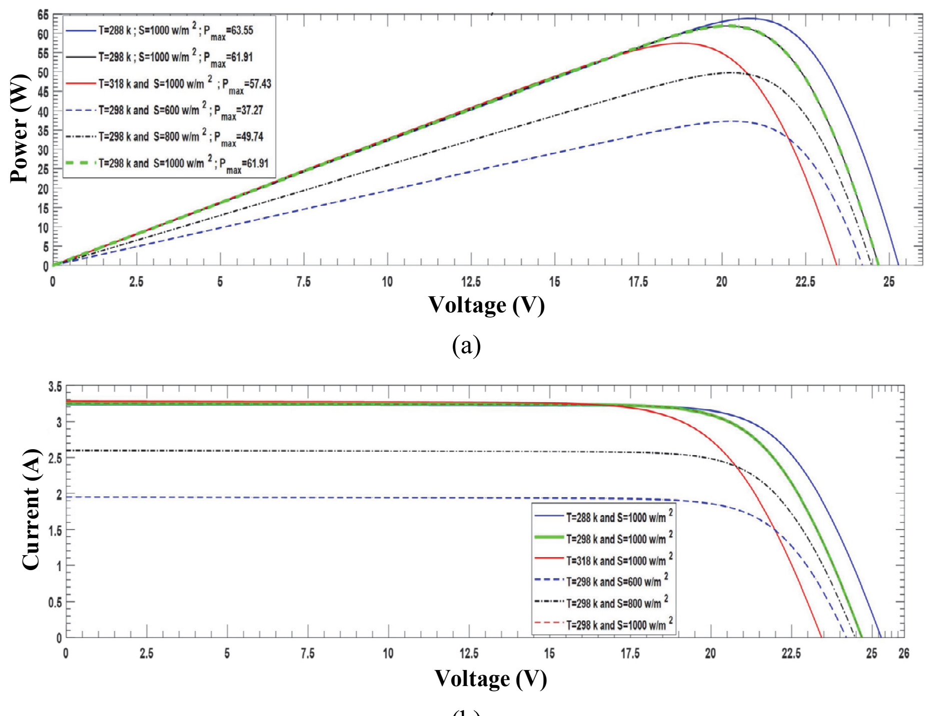

Fig. 3 – (a) p_{pv}-v_{pv}; (b) i_{pv}-v_{pv} *characteristics of the used PV module for different climatic conditions.*

The current produced by the photovoltaic cell (i_{pv}) is practically proportional to the solar irradiance S. On the other hand, the voltage v_{pv} at the terminals of the junction varies little because it is a function of the potential difference at the N-P junction of the material itself [87, 88]. The open circuit voltage only decreases slightly with irradiance. This implies that:

– The optimum module power is practically proportional to the irradiance.
– The maximum power points are approximately at the same voltage.
– The influence of the temperature on the current/voltage characteristic of a semiconductor is not negligible. For a changing temperature, it can be seen that the voltage changes much more than the current (current varies very slightly).

2.2 DC-DC boost converter

In this section, we present the principle of the DC-DC Boost converter, often used in photovoltaic systems to generate the desired voltage and current. This type of converter only consists of reactive elements, which, in the ideal case, consume no energy. For this reason, it is considered as highly efficient. Fig. 4 shows the electrical circuit of a Boost converter.

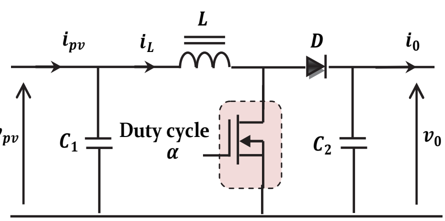

Fig. 4 – *Electrical circuit of a DC-DC Boost type converter.*

The switch (generally an IGBT or Mosfet transistor) of the boost converter is driven by a pulse width modulation (PWM) signal with a fixed frequency and a variable duty cycle α. The duty cycle is between 0 and 1, and the relationship between the input and the output voltage is expressed as a function of it:

$$\frac{v_o}{v_{pv}} = \frac{1}{1-\alpha}. \tag{6}$$

The following equation describes the approximate model of the boost converter [73] with a resistive load R:

$$\dot{v}_{pv} = \frac{i_{pv} - i_L}{C_1}, \quad \dot{i}_L = \frac{v_{pv} - (1-\alpha)v_o}{L}, \quad \dot{v}_o = \frac{(1-\alpha)i_L - i_o}{C_2}. \tag{7}$$

The values of the different components of the boost converter are calculated respecting the load consumption, which is characterized by (i_o = ~17.3 A,

$v_o = \sim 49.7$ V) at standard climatic conditions [89]. We give: $L = 3.5$ mH, $C_1 = 5.6$ mF, $C_2 = 5.6$ mF [80].

2.3 Load adaptation

As depicted in Fig. 3, the PV module strongly depends on the temperature and the irradiance changes, but also on the load value, as shown in Fig. 5. For a direct connection of the PV module with a resistive load R_o, if the slope ($1/R_o$) is much increased, the PV module will operate at its short current (I_{sc}) mode. If the slope ($1/R_o$) is much decreased, the PV module will operate at its open circuit (V_{oc}) mode. Then, the addition of the MPPT stage is indispensable to keep the PV module operating at its maximum power ($P_{pv\,(\max)}$), and the relationship between R_{pv}, R_o and the duty cycle α generated by the MPPT stage is given by $R_{pv} = (1 - \alpha)^2 R_o$ [58]. If R_o increases, α will increase to track the MPP. If R_o decreases, then α will decrease to track the MPP, Fig. 5 [58, 66].

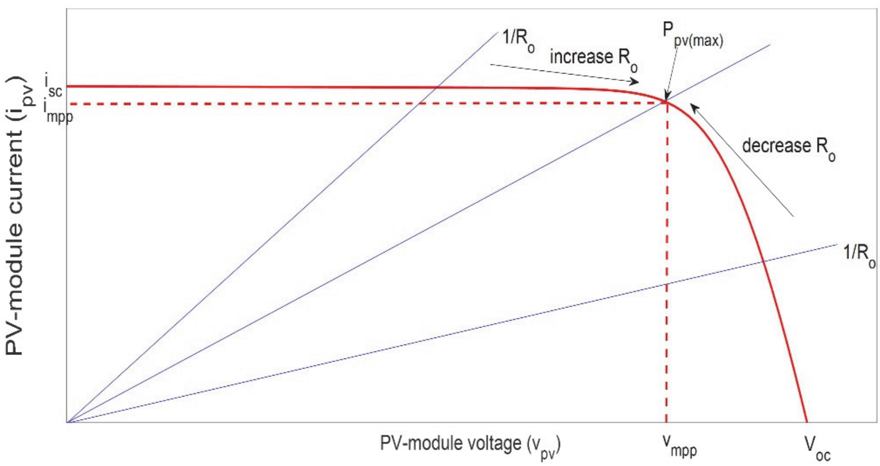

Fig. 5 – *i_{pv}-v_{pv} characteristic and load adaptation by MPPT controller stage.*

To ensure that the MPPT controller operates accurately and efficiently, non-linear loads with inverters and rectifiers connected to the grid or lead acid batteries are widely used [66, 73, 90], because the battery fulfills the role of an ideal voltage source in place of the resistor R_o, and the grid connected applications are considered in order to analyze the propagation of the 100/120 Hz perturbations from the grid to the PV-array. In this paper, the lead-acid battery presented in Fig. 6 is used, which has the transfer function:

$$TF(s) = \frac{v_o(s)}{i_o(s)} = \frac{4.2920 \cdot 10^5 s^2 + 1.3218 \cdot 10^8 s + 1.0003 \cdot 10^4}{330157100 s^2 + 4.6501 \cdot 10^7 s + 1}, \quad s = j\omega, \quad (8)$$

where the required parameters R_{bs}, R_{b1}, R_{bp}, C_{b1} and C_{bp} are reported in [65] with the following values: $R_{bs} = 0.0013\ \Omega$, $R_{b1} = 2.84\ \Omega$, $R_{bp} = 1\ \text{k}\Omega$, $C_{b1} = 2.5$ F and $C_{bp} = 4.6501$ kF.

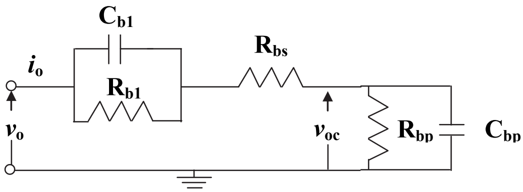

Fig. 6 – *Electric model of a lead-acid battery.*

3 MPPT Based FLC

First of all it is worth reminding that the fuzzy logic concept belongs to L. Zadeh [91]. It consists of the decomposition of the range of variation of a variable in the form of linguistic nuances such as: “small”, “Average”, “Big”, etc., and rules coming from the expertise of the human operator, which expresses, in linguistic form, how should the system controls evolve according to the observed variables. For example “IF the error is Positive Small AND the variation of the error is Positive Big THEN the variation of the output is Negative Big”. There are many manners to present the designing steps of an FLC but, in general, three steps may be considered:

Fuzzification: it is the process of transforming a measured real quantity into fuzzy sets. This is realized by many kinds of fuzzifiers (membership functions) and fuzzy rules [92].

Inference method: it employs the inference engine, which is a mechanism for condensing the information of a system through a set of rules defined for the representation of any problem. Each rule delivers a partial conclusion that is then aggregated to the other rules to provide a conclusion (aggregation). The commonly used inference method is the MAX-MIN, which is utilized in this paper [92].

Defuzzification: the center of gravity method is commonly used. This paper uses this mentioned method [92].

The design of this type of FLC-MPPT controllers is based on the power-voltage curve, which is divided into three regions, as Fig. 7 shows. The structure of the FLC-MPPT controller is given by Fig. 8. It consists of two inputs: the slope E and its variation or change CE, and one output dα, which is the change of the duty cycle α.

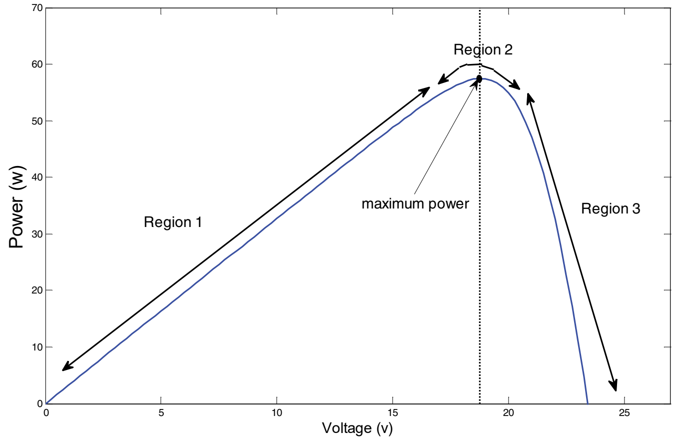

Fig. 7 – *Operation regions of a PV module in p_{pv}-v_{pv} curve.*

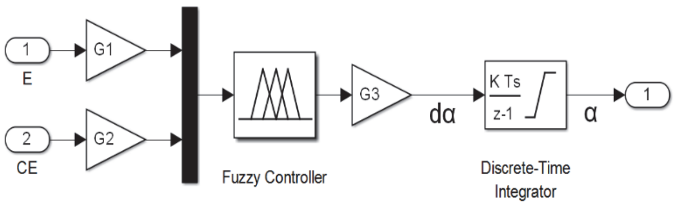

Fig. 8 – *FLC-MPPT controller structure.*

Both inputs and the output are normalized using the gains G1, G2 and G3. To obtain the duty cycle α, a discrete time integrator is used with the Forward Euler Method (the default), where the gain value K and the sample time T_s of the integrator are set to 1 and 0.01 respectively. At each step k, the duty cycle is computed as follows:

$$\alpha(k) = \alpha(k-1) + 0.01 \cdot \mathrm{d}\alpha(k-1). \tag{9}$$

Using the p_{pv}-v_{pv} slope of the PV module characteristic, the variables E and CE are expressed as follows [73]:

$$E(k) = \frac{\Delta P_{pv}}{\Delta V_{pv}} = \frac{P_{pv}(k) - P_{pv}(k-1)}{V_{pv}(k) - V_{pv}(k-1)}, \tag{10}$$

$$CE(k) = E(k) - E(k-1). \tag{11}$$

The input $E(k)$ shows whether the operating point of the PV module is located in the left (Region 1, where $E(k)$ is positive), right (Region 3, where $E(k)$ is negative) or at the maximum power (Region 2, where $E(k)$ is zeros) of the p_{pv}-v_{pv} curve, while the input $CE(k)$ is used to determine the magnitude of the duty cycle change (dα) to be increased or decreased.

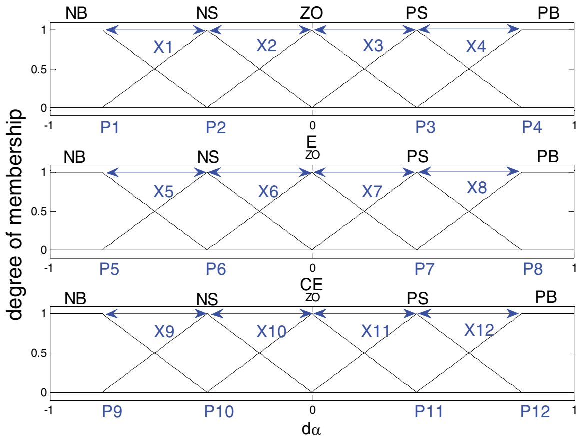

Fig. 9 – *Membership functions of FLC-MPPT controller.*

For the resolution of the problems of maximum power point tracking, the membership functions of Fig. 9 are defined using five levels of language variables such as: negative big (NB), negative small (NS), zero (ZO), positive small (PS), and positive big (PB). Conventionally, using five language variables is largely sufficient to obtain a regulation or a satisfactory trajectory tracking [93]. The forms of the chosen membership functions are shown in Fig. 9, which are suited for the easy computation and immediate solution of the optimization problems emerging in fuzzy modeling [94,95].

The parameters of the membership functions of Fig. 9 are associated by the following relations:

$$\begin{cases} P_1 = -(X_1 + X_2) \\ P_2 = -X_2 \\ P_3 = X_3 \\ P_4 = (X_3 + X_4) \end{cases} \quad \begin{cases} P_5 = -(X_5 + X_6) \\ P_6 = -X_6 \\ P_7 = X_7 \\ P_8 = (X_7 + X_8) \end{cases} \quad \begin{cases} P_9 = -(X_9 + X_{10}) \\ P_{10} = -X_{10} \\ P_{11} = X_{11} \\ P_{12} = (X_{11} + X_{12}) \end{cases} \tag{12}$$

The fuzzy rules are given in **Table 2**, where R_i ($I = 1,\ldots, 25$) can be one of the five linguistic variables (NB, NS, ZO, PS, PB). These rules are designed based on the p_{pv}-v_{pv} characteristic given in Fig. 7. For example, when the operating point is in the Region 1, the slope E is positive, so the duty cycle should be decreased with respect to CE in order to achieve the MPP; when the it is in Region 3, the slope E is negative, so the duty cycle should be increased with respect to CE in order to achieve the MPP; and when the operating point is in Region 2, the slope E and variation of the slope CE are almost zero, so the duty cycle is kept unchanged [55].

Table 2
Rules of FLC-MPPT controller.

E \ CE	NB	NS	ZO	PS	PB
NB	R_1	R_2	R_3	R_4	R_5
NS	R_6	R_7	R_8	R_9	R_{10}
ZO	R_{11}	R_{12}	R_{13}	R_{14}	R_{15}
PS	R_{16}	R_{17}	R_{18}	R_{19}	R_{20}
PB	R_{21}	R_{22}	R_{23}	R_{24}	R_{25}

NB
NS
ZO
PS
PB

Although the FLC-MPPT controller has the ability to track the MPP according to the distance between the operating point and the MPP, and the movement direction through the variable step size of the duty cycle (dα), as well as almost suppress the oscillation when the MPP is reached in certain cases, it has some drawbacks such as:

The imprecision of the MPPT at the low irradiance level.

The fluctuations and output errors that occur when Δp_{pv} and Δv_{pv} are very small, which make the slope E close to the MPP [55]. This may lead to the wrong fuzzy rule.

The modification of fuzzy membership functions may affect some fuzzy rules [76, 93]. In this paper, we propose to use the PSO algorithm to overcome this limitation, and we code the linguistic variables as NB=1, NS=2, ZO=3, PS=4, PB=5.

The maximum of the minimum (max-min) composition technique of Mamdani has been used here for the inference. Moreover, the center-of-gravity method has been used for the defuzzification process. It converts the fuzzy subset of the duty cycle step-size to real numbers, as presented in the following equation [92]:

$$\mathrm{d}\alpha = \frac{\sum_{j=1}^{n} \mu(d\alpha_j) d\alpha_j}{\sum_{j=1}^{n} \mu(d\alpha_j)}, \tag{13}$$

where $d\alpha_j$ is the center of the max–min composition at the output membership function.

4 PSO Algorithm Review

PSO is a cooperative evolutionary technique developed by Kennedy and Eberhart [96] inspired by the collective movement of animal groups. These animals can be seen as agents who have the ability to make their own decisions by imitating the successful behavior of their neighborhood while bringing their personal experience. In groups of animals, each individual moves according to his own knowledge that can be reached by the displacement of his neighbors.

4.1 Principle

This method is based on cooperation between simple individuals often called particles. These particles possess a capacity of memorization in the sense that each agent remembers his best visited position and the best position found in his neighborhood. Each particle then moves along a disturbed path between its two positions and its speed. In the case of an optimization problem, the quality of a position in the search space is determined by the value of the cost function *CF* at that point. Fig. 10 illustrates the strategy of moving a particle.

PSO is a simple and efficient algorithm that starts with a number of randomly placed particles in the search space that are initialized with random velocities.

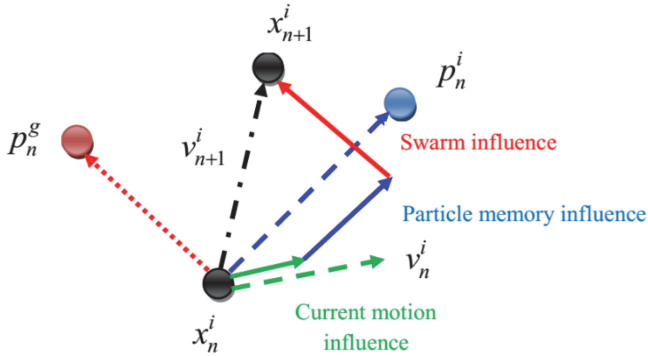

Fig. 10 – *Strategy of moving a particle in the swarm* [97].

4.2 Formalization

In a research space of dimension D, the particle i of the swarm is modeled by its vector position $X^i = (x^{i1}; x^{i2};\ldots; x^{iD})$ and by its velocity vector $V^i = (v^{i1}; v^{i2};\ldots; v^{iD})$. This particle keeps in memory the best position by which it has already passed, that we note $P^i = (p^{i1}; p^{i2};\ldots; p^{iD})$. The best position reached by all the particles of the swarm is denoted $P^g = (p^{g1}; p^{g2};\ldots; p^{gD})$. At iteration n, the position and velocity vectors are calculated by the following equations [98]:

$$v^{ij}_{(n+1)} = \chi\left[v^{ij}_n + c_1 r^{ij}_{1n}(p^{ij}_n - x^{ij}_n) + c_2 r^{ij}_{2n}(p^{gj}_n - x^{ij}_n)\right], \quad j \in \{1,\ldots,D\}, \tag{14}$$

$$x^{ij}_{(n+1)} = x^{ij}_n + v^{ij}_{(n+1)}, \quad j \in \{1,\ldots,D\}, \tag{15}$$

where r_1 and r_2 are random numbers between 0 and 1; c_1 and c_2 are positive constant learning rates; χ is called the constriction factor and is defined by the following equation [99]:

$$\chi = \frac{2}{\left|2 - c - \sqrt{c^2 - 4c}\right|}, \quad c = c_1 + c_2 . \tag{16}$$

The studies carried out by Clerc and Kennedy in [99] have shown that good convergence and prevention of the explosion of the swarm can be ensured by making the parameters χ, c_1, c_2 dependent. In the majority of cases, we use $c = 4.1$ and $c_1 = c_2$; which gives a multiplicative coefficient χ approximately equal to 0.7298.

It is possible that the displacement of a particle leads it to leave the research space of a range $[x_{\min}, x_{\max}]$. In this case, a strategy of confinement of the particles can be introduced. Such a strategy allows a particle out of the search space to return to that space as follows:

$$x^{ij} = \begin{cases} x_{\min} & \text{if} \quad x^{ij} < x_{\min} \\ x^{ij} & \text{if} \quad x_{\min} < x^{ij} < x_{\max} \\ x_{\max} & \text{if} \quad x^{ij} > x_{\max} \end{cases} . \tag{17}$$

The stopping criterion may be different depending on the problem. If the global optimum is known a priori, an "acceptable error" ε can be defined as a stop criterion. Otherwise, it is common to set a maximum number of objective function evaluations or a maximum number of iterations.

Subsequently, a flow chart of a PSO algorithm for maximization of a cost function CF (in the case of minimization, put < instead of >) is presented:

```
Random initialization of positions X^i and velocities V^i of each particle
For each particle i, P^i = X^i
while the stopping criterion is not achieved do
    For i=1 : n
        Movement of the particle using (14) and (15)
        Evaluation of positions
        If  CF(X^i) > CF(P^i)
            P^i = X^i
        end if
        If  CF(P^i) > CF(P^g)
            P^g = P^i
        end if
    end for
end while
```

4.3 Example of applications

In order to show the dependence of the PSO algorithm of its parameters, such as the dimension of the problem (D), the number of particles (M) and the number of iterations (n), a series of tests was performed on the function

$$\text{Rastrigin function}\begin{cases} F(x)=\sum_{i=1}^{D}\left(x_i^2-10\cos(2\pi x_i)+10\right) \\ x=\left[x_1,x_2,\ldots,x_D\right]\in\left[-5.12,5.12\right] \end{cases} \tag{18}$$

This function has a global optimum equal to 0. The series of tests was carried out in the following three scenarios:

1. In the first scenario, the number of iterations n and the number of particles M were fixed to 100 and 20 respectively, and the dimension of the problem D is varied.
2. In the second scenario, the number of iterations n and the dimension of the problem D were fixed to 100 and 10 respectively, and the number of particles M is varied.
3. In the third scenario, the dimension of the problem D and the number of particles M were fixed to 10 and 20 respectively, and the number of iterations n is varied.

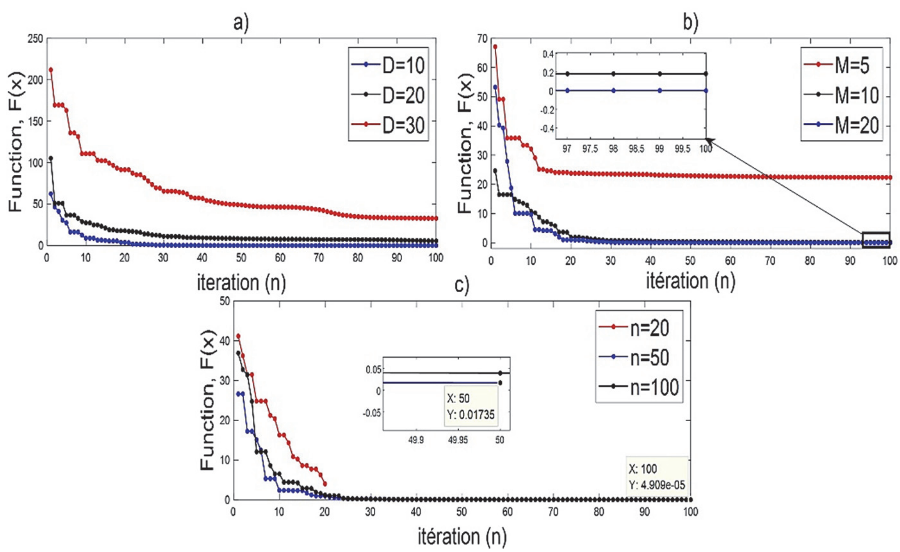

Fig. 11 – *Evolution of the function F*(x) *in the three scenarios.*

Fig. 11 shows the simulation results of a series of experiments of 5 trials. The evolution of the curves shows that:

– Increasing the dimension (D) of the problem prevents the algorithm from finding the global optimum.
– The right choice of the number of particles (M) can help to converge quickly towards the global optimum.
– Depending on the dimension of the problem (D) and the number of particles (M), it is necessary to give a sufficient number of iterations to the algorithm to converge towards the global optimum.

5 FLC-MPPT controller optimized by PSO

In this paper a FLC-MPPT controller tuned using the PSO algorithm was developed to maximize the power extraction from the PV module. The PSO algorithm was mainly used to determine the three gains G1, G2 and G3, the fuzzy subsets partitions and the shapes of the membership functions, and the fuzzy rules with respect to a predefined cost function. The whole PV-system with the tuned FLC-MPPT controller is depicted on Fig. 12.

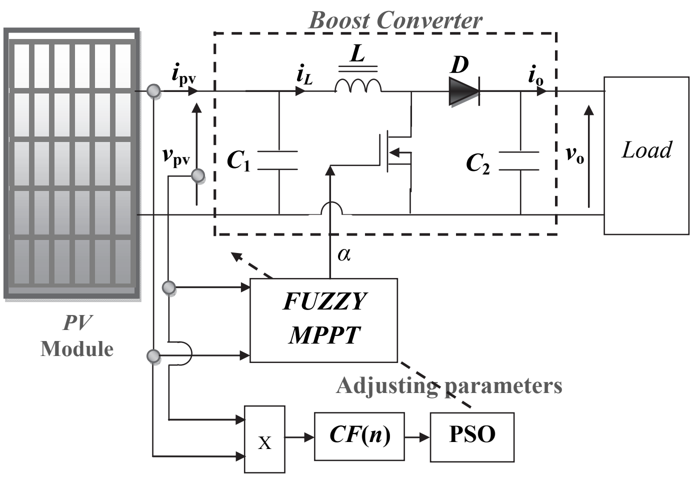

Fig. 12 – *Whole PV-system with tuning FLC-MPPT controller by PSO algorithm.*

5.1 Definition of the particle string

Before applying the PSO algorithm for searching the FLC-MPPT controller parameters, the particle string has to be defined. We have 40 controller parameters (D = 40) for one particle i (X1, X2, … ,X12, G1, G2, G3, R1, R2, …, R25). These parameters are real values that define the particle's position X^i = (X1, X2,…,X12, R1, …, R25, G1, G2, G3). If there are M particles, then the dimension of the problem is M·40.

5.2 Definition of the cost function (CF)

Many types of cost functions are used in the literature to design the controller parameters, each one having its own advantages and disadvantages [100, 101]. The commonly used ones are: the integral absolute error (IAE) [39, 102], and the integral of the squared error (ISE) [65, 66]. The IAE and ISE are expressed as follows:

$$IAE = \int \left| P_{\max}(t) - P_{pv}(t) \right| \mathrm{d}t , \tag{19}$$

$$ISE = \int \left(P_{\max}(t) - P_{pv}(t) \right)^2 \mathrm{d}t . \tag{20}$$

Numerically, these two cost functions can be expressed as:

$$IAE(n) = \sum_{k=1}^{Ns} \left| P_{\max}(k) - P_{pv}(k) \right| , \tag{21}$$

$$ISE(n) = \sum_{k=1}^{Ns} \left(P_{\max}(k) - P_{pv}(k) \right)^2 . \tag{22}$$

where $P_{\max}$ is the maximum power under a given climatic condition (temperature and irradiance), P_{pv} is the PV module power with the MPPT controller, Ns is the number of samples and n is the number of iterations. The optimization requirement is to minimize one of these two cost functions in order to track P_{pv} to $P_{\max}$. It is worth noting that the use of these functions needs the determination of $P_{\max}$ again if the optimization process has to be carried out with another profile of temperature and irradiance. To overcome this disadvantage, the maximization of the following cost function is proposed:

$$CF(n) = \sum_{k=1}^{Ns} P_{pv}(k) , \tag{23}$$

which is useful for each profile of climatic conditions.

5.3 Implementation of PSO- FLC-MPPT controller

Our implementation consists of a PSO algorithm that searches for the FLC-MPPT controller parameters including gains, membership functions and fuzzy rules. Each particle has 40 parameters. The optimization procedure is shown in the following:

Step 1. Initialize randomly the position vector X^i = (X1, X2, …., X12, G1, G2, G3, R1, …, R25), the velocity vector V^i, the best position P^i and the global best position P^g. Specify the upper and lower bounds of all the parameters, the number of particles and iterations.

Step 2. For each particle's position, calculate the cost function CF given by equation (23).

Step 3. Compare each evaluated particle's position with its best position P^i. If the current position X^i gave a higher value of CF than P^i, then assign X^i to P^i, if not, P^i remains unchanged. The best value of P^i among all the particles is denoted P^g.

Step 4. Update the velocity and the position according to (14) and (15).

Step 5. If the maximum number of iterations is reached, then go to the next step. Otherwise, go to step 2.

Step 6. The optimal set of controller parameters is the latest generated global best position P^g.

Remark 2. When the PSO algorithm stroke on a local solution for a long time and the tuning procedure cannot get-away from the local solution, a restarting optimization process is needed to keep the algorithm searching and finding from a new initial solution. Consequently, the program can be executed many times.

6 Simulation Results and Discussion

In this section, the performance of the proposed FLC-MPPT controller tuned by PSO summarized in Fig. 12 will be tested. The optimization process is done under the standard climatic condition (T = 25ºC, S = 1000 W/m^2). The optimization process is carried out with a number of particles M = 20 and a maximum number of iterations n = 30. The regions of the selective parameters are:

$$0.001 < G1, G2, G3 < 30; 0.01 < X1, X2,\ldots, X12 < 0.99 ; 1 < R1, R2, \ldots, R25 < 5.$$

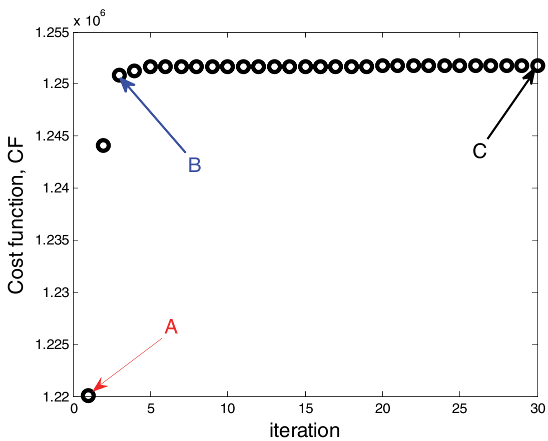

Fig. 13 – *Evolution of cost function CF Vs iteration.*

The evolution of the cost function CF (n) when the optimization algorithm is applied is given by Fig. 13. It is clear that the optimum is reached in iteration 30. In Fig. 13 points A, B and C are mentioned to show and analyze the convergence of the PV module power to the maximum power in function of the iteration number. The optimal FLC-MPPT controller membership functions, surface viewer, rules and normalization gains are given respectively by Figs. 14 and 15, together with **Tables 3** and **4**.

Table 3
Optimized fuzzy rules of FLC-MPPT.

E	CE	NB	NS	ZO	PS	PB
NB		PB	PB	NB	NB	PB
NS		PB	PB	PB	PS	NB
ZO		ZO	ZO	PB	PB	NB
PS		NB	ZO	NS	NS	PB
PB		NB	NB	NB	NB	PS

Table 4
Optimal normalization gains.

Parameter	**Value**
G1	1.0000e-03
G2	1.0000e-03
G3	0.8533

These tables show some fuzzy rules (called also inactive rules) that contradict the common sense of the MPPT control. This is the most important problem of this method, and it can be overcome by introducing, in addition to the previous cost function (CF), another objective which favors the corresponding solutions to a minimum number of active rules [93].

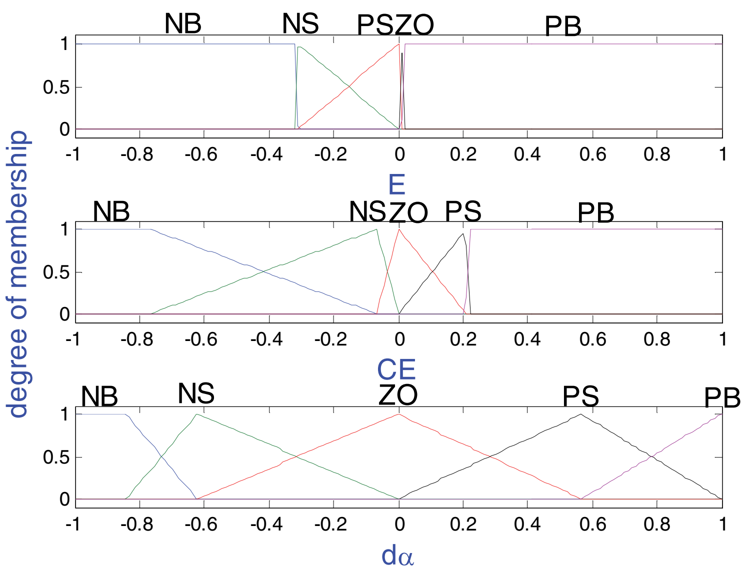

Fig. 14 – *Optimal membership functions of the FLC-MPPT controller.*

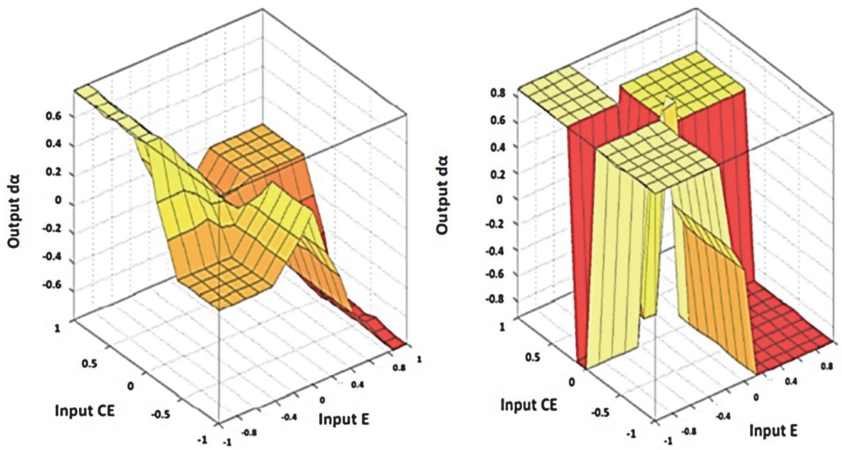

Fig. 15 – *Surface viewer for:* (a) *FLC-MPPT not optimized;*
(b) *Optimal FLC-MPPT.*

The PV system responses with the optimized FLC-MPPT controller are given by the following figures. Figs. 16a and 16b show the differences among the PV-module powers at the three different iterations A, B and C. At iteration 1 (point A), the system response presents an undershoot of 866.2 W (see the zooms of portions 1 and 2 in Figs. 16c and 16d) with respect to its steady state, which is also 866.2 W.

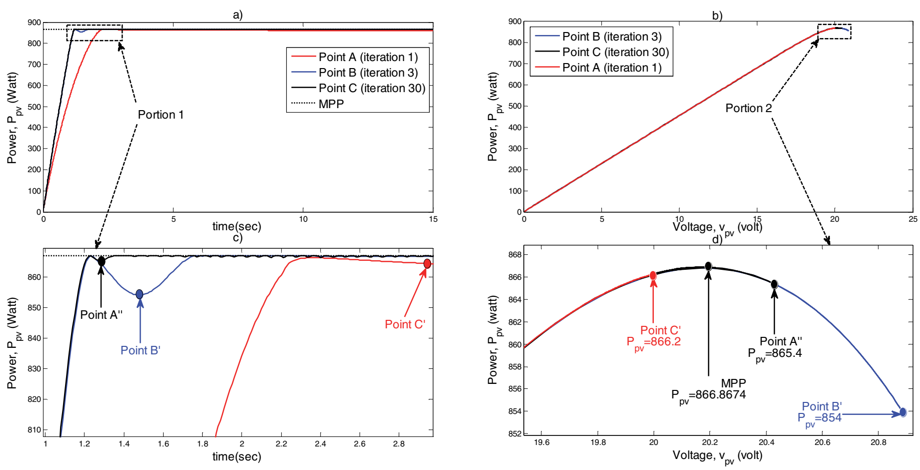

Fig. 16 – (a) *PV module power with optimized FLC-MPPT*: (b) *power-voltage curve under standard climatic condition;* (c) *zoom of portion* 1; (d) *zoom of portion 2*.

This steady state has an error of 0.6674 W with respect to the desired value. At iteration 3 (point B), the system response is almost near to the optimum. Its steady state error becomes null and the undershot is 12.8674 W. At iteration 30 (point C), the optimum is reached: the steady state error is null, the undershoot is 1.4674 W and the settling time is significantly lower than in the points A and B.

In order to test the robustness and efficiency of the optimized FLC-MPPT controller under variable values of temperature and irradiance, the following simulations are carried out. The performance of our optimized FLC-MPPT controller is also compared to the not optimized FLC-MPPT controller.

6.1 Robustness test under gradual changes in irradiance and temperature

In this scenario, both the fuzzy logic controller and the optimized FLC-MPPT controllers are performed under a variable profile of temperature and irradiance as shown in Fig. 17. This profile is generally used, e.g., [103], to test the ability of MPPT controllers to effectively deal with slope variations of the irradiance and temperature. The irradiance and temperature are set respectively to 600 W/m^2 and 298 K in the time interval [0, 15] s, and respectively to 800 W/m^2 and 288 K in the interval [40, 50] s. In the interval [15, 26] s, the irradiance increases gradually from 600 to 1000 W/m^2 and the temperature from 298 to 318 K. In the interval [35, 40] s, the irradiance decreases gradually from 1000 to 800 W/m^2 and the temperature from 318 to 288 K.

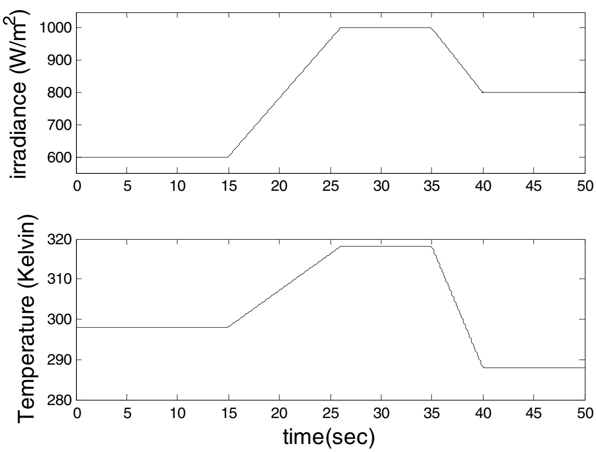

Fig. 17 – *Gradual change of irradiance and temperature.*

Fig. 18 illustrates the system response. Fig. 18a shows that the maximum power is well tracked without neither fluctuations (see the zooms of portions 3 and 4) or undershoot. This issue is clearly viewed in Fig. 18b, where the optimum PV module voltage under changing temperature and irradiance is also well tracked. Such optimum point is closely tracked from $P_{max(1)}$ to $P_{max(2)}$ and then to $P_{max(3)}$ with small oscillations (see the zoom of portion 5). These figures show that this performance is not reached if the FLC-MPPT controller without optimization is used.

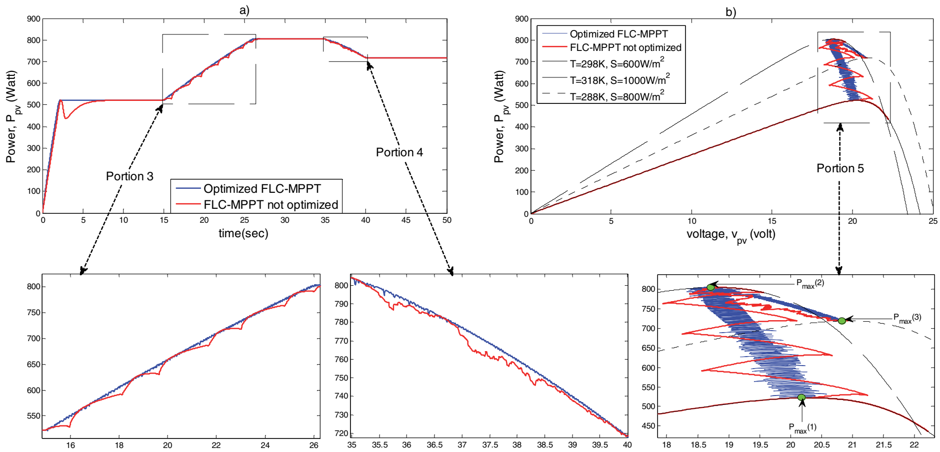

Fig. 18 – (a) *PV module power with optimized FLC-MPPT under the variable profile of temperature and irradiance;* (b) *power-voltage curve.*

6.2 Robustness test under real changes of irradiance and temperature

In this scenario, the MPPT techniques are simulated using the real daily profile of irradiance and temperature shown in Fig. 19. The data of irradiance and temperature were collected by the "Unité de Recherche Appliquée en Energies Renouvelable, in Ghardaïa, Algeria" on November 05, 2012 [104], using the K&Z CHP1 Pyrheliometer and Campbell CS21 tools. This choice allows us to assess the effect of using MPPT controllers in the PV system as well as the differences in performance between them. The changes of irradiance and temperature are almost proportional to the morning day time until 12:00h. From 12:00h to 15:00h, the irradiance varies between 814 and 844 W/m^2 and the temperature still increases until 33ºC, beginning from 30ºC at 12:00h. After 15:00h, the irradiance decreases until 160 W/m^2 at 18:00h while the temperature remains constant between 15:00h and 17:00h, decreasing after that as a consequence of the sunset.

The simulation results of this scenario are given in Fig. 20. Fig. 20a shows that the performance of the optimized FLC-MPPT controller surpasses the not optimized FLC-MPPT controller. This last controller presents clear power drops at 09:15h and 10:17h, which are caused by the violation of the PV module voltage (see Fig. 20b) around the optimum voltage.

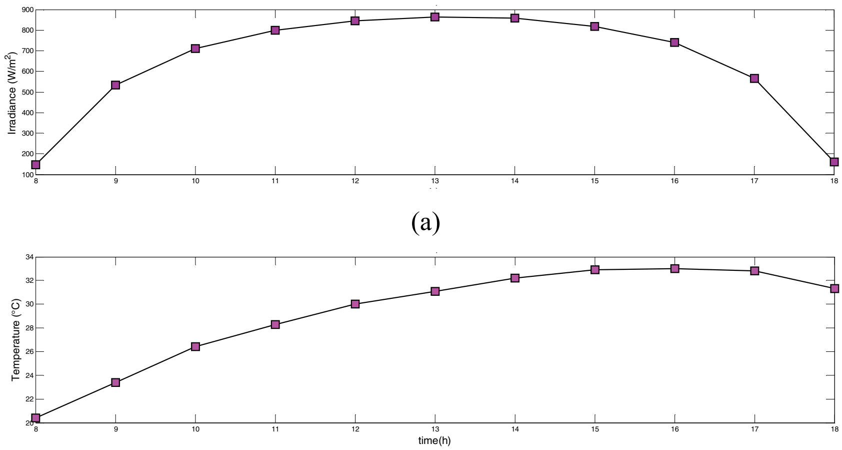

(a)

(b)

Fig. 19 – *Real daily profile of:* (a) *irradiance;* (b) *temperature.*

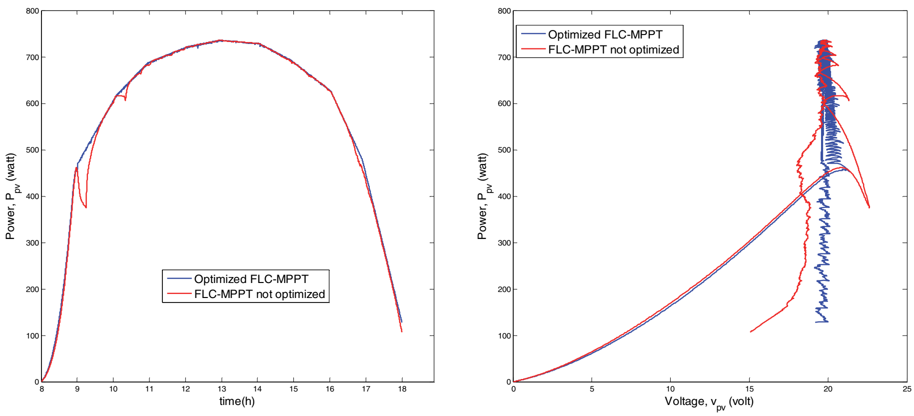

(a) (b)

Fig. 20 – (a) *PV module power with optimized FLC-MPPT under the real daily profile of temperature and irradiance;* (b) *power-voltage curve.*

6.3 Comparison

In order to make a fairer comparison, the efficiency E_f given by

$$E_f = \frac{\sum_{i=1}^{N} p_{MPPT}(i)}{\sum_{i=1}^{N} p_{max}(i)} \cdot 100 \tag{24}$$

is considered. It is based on the efficiency calculated as the quotient between the output power of the photovoltaic system with the MPPT controller and the output power at the true MPP (P_{max}), in which N is the number of samples.

Table 5
Efficiency of the FLC-MPPT techniques in all simulated cases.

	FLC-MPPT controller	FLC-MPPT controller with optimized normalization gains	FLC-MPPT controller with optimized normalization gains and membership functions	Proposed optimized FLC-MPPT controller
Standard climatic condition	94.32 %	**96.24** %	96.23 %	96.15 %
Gradual change in irradiance and temperature	97.72 %	98.17 %	98.23 %	**98.53** %
Real change of irradiance and temperature	96.93 %	96.94 %	97.67 %	**97.87** %

The proposed optimized FLC-MPPT controller is compared to the not optimized FLC-MPPT controller, the FLC-MPPT controller with optimized normalization gains, and the FLC-MPPT controller with optimized normalization gains and membership functions.

The numerical results given in **Table 5** show the superior performance of the FLC-MPPT controller with optimized normalization gains in the standard climatic condition, but the improvement achieved with respect to the other approaches is small (only of 0.09 % with respect to our proposal). The slightly weaker performance of our controller can be explained by an excessive number of parameters to be optimized in this case, since the increase of the dimension of the optimization problem can prevent the algorithm from finding the global optimal solution (as discussed in Section 4–3). Increasing the number of iterations over the established 30 can solve this problem. In the other two scenarios, the proposed optimized FLC-MPPT controller has given the best performance index.

7 Conclusion

In this paper, a methodology for designing the FLC parameters based on a PSO algorithm for the maximum power point tracking of a PV has been introduced. The FLC-MPPT controller gains, membership functions and rules are iteratively adjusted by the PSO algorithm in order to maximize a cost function based on the PV module power under the standard climatic conditions (T=25ºC and S=1000 W/m^2). The comparison under different scenarios of this optimized FLC-MPPT controller, the not optimized FLC-MPPT controller, the FLC-MPPT controller with optimized normalization gains and the FLC-MPPT controller with optimized normalization gains and membership functions has shown the superiority of the first one in most of the studied cases.

The proposed optimized FLC-MPPT controller achieves a short settling time, small oscillations around the MPP and no steady state error. However, our optimization procedure may yield fuzzy rules that contradict the common sense of the MPPT controllers. This can be overcome by introducing another additional objective that favors the minimum number of active fuzzy rules. This is the perspective of our next work.

8 Acknowledgments

This project was financially supported by the Directorate General for Scientific Research and Technological Development – Algerian Ministry of Higher Education and Scientific Research.

9 References

[1] N. Femia, G. Petrone, G. Spagnuolo, M. Vitelli: Optimization of Perturb and Observe Maximum Power Point Tracking Method, IEEE Transactions on Power Electronics, Vol. 20, No. 4, July 2005, pp. 963 – 973.

[2] A. Ilyas, M. Ayyub, M.R. Khan, M. A. Husain, A. Jain: Hardware Implementation of Perturb and Observe Maximum Power Point Tracking Algorithm for Solar Photovoltaic System, Transactions on Electrical and Electronic Materials, Vol. 19, No. 3, June 2018, pp. 222 – 229.

[3] M. Berrera, A. Dolara, R. Faranda, S. Leva: Experimental Test of Seven Widely-Adopted MPPT Algorithms, Proceedings of the IEEE PowerTech, Bucharest, Romania, June 2009, pp. 1 – 8.

[4] F. Liu, Y. Kang, Y. Zhang, S. Duan: Comparison of P&O and Hill Climbing MPPT Methods for Grid-Connected PV Converter, Proceedings of the 3rd IEEE Conference on Industrial Electronics and Applications (ICIEA), Singapore, Singapore, June 2008, pp. 804 – 807.

[5] T.- C. Yu, Y.- C. Lin: A Study on Maximum Power Point Tracking Algorithms for Photovoltaic Systems, Journal of Longhua, No. 30, December 1999, pp. 27 – 36.

[6] K.H. Hussein, I. Muta, T. Hoshino, M. Osakada: Maximum Photovoltaic Power Tracking: An Algorithm for Rapidly Changing Atmospheric Conditions, IEE Proceedings-Generation, Transmission and Distribution, Vol. 142, No. 1, January 1995, pp. 59 – 64.

[7] L. Suganthi, S. Iniyan, A.A. Samuel: Applications of Fuzzy Logic in Renewable Energy Systems – A Review, Renewable and Sustainable Energy Reviews, Vol. 48, August 2015, pp. 585 – 607.

[8] Y.- T. Chen, Y.- C. Jhang, R.- H. Liang: A Fuzzy-Logic Based Auto-Scaling Variable Step-Size MPPT Method for PV Systems, Solar Energy, Vol. 126, March 2016, pp. 53 – 63.

[9] T. Radjai, L. Rahmani, S. Mekhilef, J. P. Gaubert: Implementation of a Modified Incremental Conductance MPPT Algorithm with Direct Control based on a Fuzzy Duty Cycle Change Estimator Using dSPACE, Solar Energy, Vol. 110, December 2014, pp. 325 – 337.

[10] T. Radjai, J.P. Gaubert, L. Rahmani, S. Mekhilef: Experimental Verification of P&O MPPT Algorithm with Direct Control based on Fuzzy Logic Control Using CUK Converter, International Transactions on Electrical Energy Systems, Vol. 25, No. 12, December 2015, pp. 3492 – 3508.

[11] A. Al Nabulsi, R. Dhaouadi: Efficiency Optimization of a DSP-Based Standalone PV System Using Fuzzy Logic and Dual-MPPT Control, IEEE Transactions on Industrial Informatics, Vol. 8, No. 3, August 2012, pp. 573 – 584.

[12] A. El Khateb, N. Abd Rahim, J. Selvaraj, M.N. Uddin: Fuzzy-Logic-Controller-Based SEPIC Converter for Maximum Power Point Tracking, IEEE Transactions on Industry Applications, Vol. 50, No. 4, July 2014, pp. 2349 – 2358.

[13] I.H. Altas, A.M. Sharaf: A Novel Maximum Power Fuzzy Logic Controller for Photovoltaic Solar Energy Systems, Renewable Energy, Vol. 33, No. 3, March 2008, pp. 388 – 399.

[14] I.H. Altas, A.M. Sharaf: A Fuzzy Logic Power Tracking Controller for a Photovoltaic Energy Conversion Scheme, Electric Power Systems Research, Vol. 25, No. 3, December 1992, pp. 227 – 238.

[15] C. Ben Salah, M. Ouali: Comparison of Fuzzy Logic and Neural Network in Maximum Power Point Tracker for PV Systems, Electric Power Systems Research, Vol. 81, No. 1, January 2011, pp. 43 – 50.

[16] M.S. Aït Cheikh, C. Larbes, G.F. Tchoketch Kebir, A. Zerguerras: Maximum Power Point Tracking Using a Fuzzy Logic Control Scheme, Revue des Energies Renouvelables, Vol. 10, No. 3, September 2007, pp. 387 – 395.

[17] Y.- Y. Hong, A.A. Beltran, A.C. Paglinawan: Real-Time Simulation of Maximum Power Point Tracking Control Using Fuzzy Logic for Stand Alone PV System, Proceedings of the IEEE 3rd International Future Energy Electronics Conference and ECCE Asia (IFEEC 2017-ECCE Asia), Kaohsiung, Taiwan, June 2017, pp. 710 – 715.

[18] A. Menadi, S. Abdeddaim, A. Betka, M.T. Benchouia: Real Time Implementation of A Fuzzy Logic Based MPPT Controller for Grid Connected Photovoltaic System, International Journal of Renewable Energy Research, Vol. 5, No. 1, March 2015, pp. 236 – 244.

[19] B.K. Naick, T.K. Chatterjee, K. Chatterjee: Performance Analysis of Maximum Power Point Tracking Algorithms Under Varying Irradiation, International Journal of Renewable Energy Development, Vol. 6, No. 1, March 2017, pp. 65 – 74.

[20] H. Mahamudul, M. Saad, M. Ibrahim Henk: Photovoltaic System Modeling with Fuzzy Logic Based Maximum Power Point Tracking Algorithm, International Journal of Photoenergy, Vol. 2013, ID 762946, September 2013, pp. 1 – 10.

[21] F. Bouchafaa, I. Hamzaoui, A. Hadjammar: Fuzzy Logic Control for the Tracking of Maximum Power Point of a PV System, Energy Procedia, Vol. 6, April 2011, pp. 633 – 642.

[22] M. Adly, H. El-Sherif, M. Ibrahim: Maximum Power Point Tracker for a PV Cell Using a Fuzzy Agent Adapted by the Fractional Open Circuit Voltage Technique, Proceedings of the IEEE International Conference on Fuzzy Systems (FUZZ-IEEE 2011), Taipei, Taiwan, June 2011, pp. 1918 – 1922.

[23] A. Al-Gizi, S. Al-Chlaihawi, A. Craciunescu: Efficiency of Photovoltaic Maximum Power Point Tracking Controller based on a Fuzzy Logic, Advances in Science, Technology and Engineering Systems Journal (ASTES), Vol. 2, No. 3, July 2017, pp. 1245 – 1251.

[24] A. Messai, A. Mellit, A. Massi Pavan, A. Guessoum, H. Mekki: FPGA-Based Implementation of a Fuzzy Controller (MPPT) for Photovoltaic Module, Energy Conversion and Management, Vol. 52, No. 7, July 2011, pp. 2695 – 2704.

[25] A.M. Othman, M.M.M. El-arini, A. Ghitas, A. Fathy: Realworld Maximum Power Point Tracking Simulation of PV System based on Fuzzy Logic Control, NRIAG Journal of Astronomy and Geophysics, Vol. 1, No. 2, December 2012, pp. 186 – 194.

[26] S.M. Reza Tousi, M.H. Moradi, A. Bahrami: A Fuzzy Maximum Power Point Tracking Method for Photovoltaic Systems Using a Single Input Current Sensor, IEEJ Transactions on Electrical and Electronic Engineering, Vol. 11, No. 6, November 2016, pp. 700 – 707.

[27] E.N. Yaqin, A.G. Abdullah, D.L. Hakim, A.B.D. Nandiyanto: MPPT based on Fuzzy Logic Controller for Photovoltaic System Using PSIM and Simulink, IOP Conference Series: Materials Science and Engineering, Vol. 288, January 2018, 012066, pp. 1 – 12.

[28] U. Yilmaz, A. Kircay, S. Borekci: PV System Fuzzy Logic MPPT Method and PI Control as a Charge Controller, Renewable and Sustainable Energy Reviews, Vol. 81, No. 1, January 2018, pp. 994 – 1001.

[29] A. Youssef, M. El Telbany, A. Zekry: Reconfigurable Generic FPGA Implementation of Fuzzy Logic Controller for MPPT of PV Systems, Renewable and Sustainable Energy Reviews, Vol. 82, No. 1, February 2018, pp. 1313 – 1319.

[30] M.M. Algazar, H. AL-monier, H. Abd EL-halim, M.E. El Kotb Salem: Maximum Power Point Tracking Using Fuzzy Logic Control, International Journal of Electrical Power & Energy Systems, Vol. 39, No. 1, July 2012, pp. 21 – 28.

[31] B. Bendib, F. Krim, H. Belmili, M.F. Almi, S. Boulouma: Advanced Fuzzy MPPT Controller for a Stand-Alone PV System, Energy Procedia, Vol. 50, June 2014, pp. 383 – 392.

[32] H. Abbes, H. Abid, K. Loukil, A. Toumi, M. Abid: Etude Comparative De Cinq Algorithmes De Commande Mppt Pour Un Système Photovoltaïque, Revue des Energies Renouvelables, Vol. 17, No. 3, September 2014, pp. 435 – 445.

[33] H. Bounechba, A. Bouzid, K. Nabti, H. Benalla: Comparison of Perturb & Observe and Fuzzy Logic in Maximum Power Point Tracker for PV Systems, Energy Procedia, Vol. 50, June 2014, pp. 677 – 684.

[34] J.V. Lagudu, G. Vulasala, S. Sathy Narayana: Maximum Energy Harvesting in Solar Photovoltaic System Using Fuzzy Logic Technique, International Journal of Ambient Energy, Vol. 42, No. 2, October 2018, pp. 131 – 139.

[35] R.M. Asif, A. Ur Rehman, S. Ur Rehman, J. Arshad, J. Hamid, M. Tariq Sadiq, S. Tahir: Design and Analysis of Robust Fuzzy Logic Maximum Power Point Tracking Based Isolated Photovoltaic Energy System, Engineering Reports, Vol. 2, No. 9, September 2020, e12234, pp. 1 – 16.

[36] W. Na, P. Chen, J. Kim: An Improvement of a Fuzzy Logic-Controlled Maximum Power Point Tracking Algorithm for Photovoltaic Applications, Applied Sciences, Vol. 7, No. 4, March 2017, 326, pp. 1 – 17.

[37] S.D. Al-Majidi, M F. Abbod, H.S. Al-Raweshidy: A Novel Maximum Power Point Tracking Technique based on Fuzzy Logic for Photovoltaic Systems, International Journal of Hydrogen Energy, Vol. 43, No. 31, August 2018, pp. 14158 – 14171.

[38] S. Ozdemir, N. Altin, I. Sefa: Fuzzy Logic Based MPPT Controller for High Conversion Ratio Quadratic Boost Converter, International Journal of Hydrogen Energy, Vol. 42, No. 28, July 2017, pp. 17748 – 17759.

[39] A. Borni, N. Bouarroudj, A. Bouchakour, L. Zaghba: P&O-PI and Fuzzy-PI MPPT Controllers and their Time Domain Optimization Using PSO and GA for Grid-Connected

Photovoltaic System: A Comparative Study, International Journal of Power Electronics, Vol. 8, No. 4, June 2017, pp. 300 – 322.

[40] A.H. El Khateb, N. Abd Rahim, J. Selvaraj: Fuzzy Logic Control Approach of a Maximum Power Point Employing SEPIC Converter for Standalone Photovoltaic System, Procedia Environmental Sciences, Vol. 17, 2013, pp. 529 – 536.

[41] B. N. Alajmi, K. H. Ahmed, S. J. Finney, B. W. Williams: Fuzzy-Logic-Control Approach of a Modified Hill-Climbing Method for Maximum Power Point in Microgrid Standalone Photovoltaic System, IEEE Transactions on Power Electronics, Vol. 26, No. 4, April 2011, pp. 1022 – 1030.

[42] B. Boukezata, A. Chaoui, J.- P. Gaubert, M. Hachemi: An Improved Fuzzy Logic Control MPPT Based P&O Method to Solve Fast Irradiation Change Problem, Journal of Renewable and Sustainable Energy, Vol. 8, No. 4, July 2016, 043505, pp. 1 – 14.

[43] P. Takun, S. Kaitwanidvilai, C. Jettanasen: Maximum Power Point Tracking Using Fuzzy Logic Control for Photovoltaic Systems, Proceedings of the International MultiConference of Engineers and Computer Scientists (IMECS 2011), Hong Kong, China, March 2011, pp. 986 – 990.

[44] A.M. Noman, K.E. Addoweesh, H.M. Mashaly: A fuzzy Logic Control Method for MPPT of PV Systems, Proceedings of the 38th Annual Conference on IEEE Industrial Electronics Society, Montreal, Canada, October 2012, pp. 874 – 880.

[45] S. Subiyanto, A. Mohamed, M.A. Hannan: Maximum Power Point Tracking in Grid Connected PV System Using a Novel Fuzzy Logic Controller, Proceedings of the IEEE Student Conference on Research and Development (SCOReD), Serdang, Malaysia, November 2009, pp. 349 – 352.

[46] M.A.A. Mohd Zainuri, M.A. Mohd Radzi, A.C. Soh, N. Abd Rahim: Development of Adaptive Perturb and Observe-Fuzzy Control Maximum Power Point Tracking for Photovoltaic Boost DC–DC Converter, IET Renewable Power Generation, Vol. 8, No. 2, March 2014, pp. 183 – 194.

[47] T. Boutabba, S. Drid, L. Chrifi-Alaoui, M. Benbouzid: A New Implementation of Maximum Power Point Tracking based on Fuzzy Logic Algorithm for Solar Photovoltaic System, International Journal of Engineering – Transactions A: Basics, Vol. 31, No. 4, April 2018, pp. 580 – 587.

[48] M. Nabipour, M. Razaz, S. G. H. Seifossadat, S. S. Mortazavi: A New MPPT Scheme based on a Novel Fuzzy Approach, Renewable and Sustainable Energy Reviews, Vol. 74, July 2017, pp. 1147 – 1169.

[49] T.H. Kwan, X. Wu: Maximum Power Point Tracking Using a Variable Antecedent Fuzzy Logic Controller, Solar Energy, Vol. 137, November 2016, pp. 189 – 200.

[50] S. Tang, Y. Sun, Y. Chen, Y. Zhao, Y. Yang, W. Szeto: An Enhanced MPPT Method Combining Fractional-Order and Fuzzy Logic Control, IEEE Journal of Photovoltaics, Vol. 7, No. 2, March 2017, pp. 640 – 650.

[51] B.N. Alajmi, K. H. Ahmed, S.J. Finney, B.W. Williams: A Maximum Power Point Tracking Technique for Partially Shaded Photovoltaic Systems in Microgrids, IEEE Transactions on Industrial Electronics, Vol. 60, No. 4, April 2013, pp. 1596 – 1606.

[52] L. Liu, C. Liu, J. Wang, Y. Kong: Simulation and Hardware Implementation of a Hill-Climbing Modified Fuzzy-Logic for Maximum Power Point Tracking with Direct Control Method Using Boost Converter, Journal of Vibration and Control, Vol. 21, No. 2, February 2015, pp. 335 – 342.

[53] R. Rajesh, M. C. Mabel: Design and Real time Implementation of a Novel Rule Compressed Fuzzy Logic Method for the Determination Operating Point in a Photo Voltaic System, Energy, Vol. 116, No. 1, December 2016, pp. 140 – 153.

[54] X. Li, H. Wen, Y. Hu, L. Jiang: A Novel Beta Parameter Based Fuzzy-Logic Controller for Photovoltaic MPPT Application, Renewable Energy, Vol. 130, January 2019, pp. 416 – 427.

[55] J.- K. Shiau, Y.- C. Wei, B.- C. Chen: A Study on the Fuzzy-Logic-Based Solar Power MPPT Algorithms Using Different Fuzzy Input Variables, Algorithms, Vol. 8, No. 2, June 2015, pp. 100 – 127.

[56] R. Guruambeth, R. Ramabadran: Fuzzy Logic Controller for Partial Shaded Photovoltaic Array Fed Modular Multilevel Converter, IET Power Electronics, Vol. 9, No. 8, June 2016, pp. 1694 – 1702.

[57] A. Al Nabulsi, R. Dhaouadi, H.- U. Rehman: Single Input Fuzzy Controller (SFLC) Based Maximum Power Point Tracking, Proceedings of the 4th International Conference on Modeling, Simulation and Applied Optimization (ICMSAO), Kuala Lumpur, Malaysia, April 2011, pp. 1 – 5.

[58] M. Farhat, O. Barambones, L. Sbita: Efficiency Optimization of a DSP-Based Standalone PV System Using a Stable Single Input Fuzzy Logic Controller, Renewable and Sustainable Energy Reviews, Vol. 49, September 2015, pp. 907 – 920.

[59] B. Benlahbib, N. Bouarroudj, S. Mekhilef, T. Abdelkrim, A. Lakhdari, F. Bouchafaa: A Fuzzy Logic Controller based on Maximum Power Point Tracking Algorithm for Partially Shaded PV Array-Experimental Validation, Elektronika ir Elektrotechnika, Vol. 24, No. 4, August 2018, pp. 38 – 44.

[60] S.- a. Blaifi, S. Moulahoum, R. Benkercha, B. Taghezouit, A. Saim: M5P Model Tree Based Fast Fuzzy Maximum Power Point Tracker, Solar Energy, Vol. 163, March 2018, pp. 405 – 424.

[61] C.- L. Liu, J.- H. Chen, Y.- H. Liu, Z.- Z. Yang: An Asymmetrical Fuzzy-Logic-Control-Based MPPT Algorithm for Photovoltaic Systems, Energies, Vol. 7, No. 4, April 2014, pp. 2177 – 2193.

[62] O. Guenounou, B. Dahhou, F. Chabour: Adaptive Fuzzy Controller Based MPPT for Photovoltaic Systems, Energy Conversion and Management, Vol. 78, February 2014, pp. 843 – 850.

[63] M. Adly, A.H. Besheer: An Optimized Fuzzy Maximum Power Point Tracker for Stand Alone Photovoltaic Systems: Ant Colony Approach, Proceedings of the 7th IEEE Conference on Industrial Electronics and Applications (ICIEA), Singapore, Singapore, July 2012, pp. 113 – 119.

[64] A. Hadjaissa, K. Ameur, M.S. Ait-Cheikh, N. Essounbouli: A PSO-Based Optimization of a Fuzzy-Based MPPT Controller for a Photovoltaic Pumping System Used for Irrigation of Greenhouses, Iranian Journal of Fuzzy Systems, Vol. 13, No. 3, May 2016, pp. 1– 18.

[65] F. Chekired, A. Mellit, S.A. Kalogirou, C. Larbes: Intelligent Maximum Power Point Trackers for Photovoltaic Applications Using FPGA Chip: A Comparative Study, Solar Energy, Vol. 101, March 2014, pp. 83 – 99.

[66] C. Larbes, S.M. Aït Cheikh, T. Obeidi, A. Zerguerras: Genetic Algorithms Optimized Fuzzy Logic Control for the Maximum Power Point Tracking in Photovoltaic System, Renewable Energy, Vol. 34, No. 10, October 2009, pp. 2093 – 2100.

[67] A. Messai, A. Mellit, A. Guessoum, S.A. Kalogirou: Maximum Power Point Tracking Using a GA Optimized Fuzzy Logic Controller and Its FPGA Implementation, Solar Energy, Vol. 85, No. 2, February 2011, pp. 265 – 277.

[68] S. Subiyanto, A. Mohamed, M.A. Hannan: Intelligent Maximum Power Point Tracking for PV System Using Hopfield Neural Network Optimized Fuzzy Logic Controller, Energy and Buildings, Vol. 51, August 2012, pp. 29 – 38.

[69] N. Khaehintung, A. Kunakorn, P. Sirisuk: A Novel Fuzzy Logic Control Technique Tuned by Particle Swarm Optimization for Maximum Power Point Tracking for a Photovoltaic System Using a Current-Mode Boost Converter with Bifurcation Control, International Journal of Control, Automation and Systems, Vol. 8, No. 2, April 2010, pp. 289 – 300.

[70] L.K. Letting, J.L. Munda, Y. Hamam: Optimization of a Fuzzy Logic Controller for PV Grid Inverter Control Using S-Function Based PSO, Solar Energy, Vol. 86, No. 6, June 2012, pp. 1689 – 1700.

[71] H. Abu-Rub, A. Iqbal, S. M. Ahmed, F. Z. Peng, Y. Li, G. Baoming: Quasi-Z-Source Inverter-Based Photovoltaic Generation System with Maximum Power Tracking Control Using ANFIS, IEEE Transactions on Sustainable Energy, Vol. 4, No. 1, January 2013, pp. 11 – 20.

[72] P.- C. Cheng, B.- R. Peng, Y.- H. Liu, Y.- S. Cheng, J.- W. Huang: Optimization of a Fuzzy-Logic-Control-Based MPPT Algorithm Using the Particle Swarm Optimization Technique, Energies, Vol. 8, No. 6, June 2015, pp. 5338 – 5360.

[73] N. Bouarroudj, D. Boukhetala, A. Djari, Y. Rais, B. Benlahbib: FLC Based Gaussian Membership Functions Tuned by PSO and GA for MPPT of Photovoltaic System: A Comparative Study, Proceedings of the 6th International Conference on Systems and Control (ICSC), Batna, Algeria, May 2017, pp. 317 – 322.

[74] A. Bouchakour, A. Borni, M. Brahami: Comparative Study of P&O-PI and Fuzzy-PI MPPT Controllers and their Optimization Using GA and PSO for Photovoltaic Water Pumping Systems, International Journal of Ambient Energy, Vol. 42, No. 15, May 2019, pp. 1746 – 1757.

[75] T.L. Kottas, Y.S. Boutalis, A.D. Karlis: New Maximum Power Point Tracker for PV Arrays Using Fuzzy Controller in Close Cooperation with Fuzzy Cognitive Networks, IEEE Transactions on Energy Conversion, Vol. 21, No. 3, September 2006, pp. 793 – 803.

[76] N. Patcharaprakiti, S. Premrudeepreechacharn, Y. Sriuthaisiriwong: Maximum Power Point Tracking Using Adaptive Fuzzy Logic Control for Grid-Connected Photovoltaic System, Renewable Energy, Vol. 30, No. 11, September 2005, pp. 1771 – 1788.

[77] P.K. Nayak, S. Mahesh, H.J. Snaith, D. Cahen: Photovoltaic Solar Cell Technologies: Analysing the State of the Art, Nature Reviews Materials, Vol. 4, No. 4, April 2019, pp. 269 – 285.

[78] T. Ahmad, S. Sobhan, M.F. Nayan: Comparative Analysis between Single Diode and Double Diode Model of PV Cell: Concentrate Different Parameters Effect on Its Efficiency, Journal of Power and Energy Engineering, Vol. 4, No. 3, March 2016, pp. 31 – 46.

[79] N.M. Abd Alrahim Shannan, N.Z. Yahaya, B. Singh: Single-Diode Model and Two-Diode Model of PV Modules: A Comparison, Proceedings of the IEEE International Conference on Control System, Computing and Engineering (ICCSCE), Penang, Malaysia, November 2013, pp. 210 – 214.

[80] M.S. Ait Cheikh: Study, investigation and design of control algorithms applied to photovoltaic systems, Ph.D. Thesis, Ecole National Polytechnique, Algiers, 2007. (In French).

[81] V.J. Chin, Z. Salam, K. Ishaque: Cell Modelling and Model Parameters Estimation Techniques for Photovoltaic Simulator Application: A Review, Applied Energy, Vol. 154, September 2015, pp. 500 – 519.

[82] B. Romero, G. del Pozo, B. Arredondo: Exact Analytical Solution of a Two Diode Circuit Model for Organic Solar Cells Showing S-Shape Using Lambert W-Functions, Solar Energy, Vol. 86, No. 10, October 2012, pp. 3026 – 3029.

[83] M. Q. Duong, H.H. Nguyen, S. Leva, M. Mussetta, G. N. Sava, S. Costinas: Performance Analysis of a 310Wp Photovoltaic Module based on Single and Double Diode Model, Proceedings of the International Symposium on Fundamentals of Electrical Engineering (ISFEE), Bucharest, Romania, June 2016, pp. 1 – 6.

[84] G.H. Yordanov, O.- M. Midtgård, T. O. Saetre: Two-Diode Model Revisited: Parameters Extraction from Semi-Log Plots of I-V Data, Proceedings of the 25th European Photovoltaic Solar Energy Conference and Exhibition/5th World Conference on Photovoltaic Energy Conversion, Valencia, Spain, September 2010, pp. 4156 – 4163.

[85] V. Franzitta, A. Orioli, A. Di Gangi: Assessment of the Usability and Accuracy of Two-Diode Models for Photovoltaic Modules, Energies, Vol. 10, No. 4, April 2017, 564, pp. 1 – 32.

[86] K. Et-torabi, I. Nassar-eddine, A. Obbadi, Y. Errami, R. Rmaily, S. Sahnoun, A. El fajri, M. Agunaou: Parameters Estimation of the Single and Double Diode Photovoltaic Models Using a Gauss–Seidel Algorithm and Analytical Method: A Comparative Study, Energy Conversion and Management, Vol. 148, September 2017, pp. 1041 – 1054.

[87] H. J. Möller: Semiconductors for Solar Cells, Artech House Publishers, Boston, 1993.

[88] B. van der Zwaan, A. Rabl: Prospects for PV: A Learning Curve Analysis, Solar Energy, Vol. 74, No. 1, January 2003, pp. 19 – 31.

[89] S.K. Kollimalla, M.K. Mishra: A Novel Adaptive P&O MPPT Algorithm Considering Sudden Changes in the Irradiance, IEEE Transactions on Energy Conversion, Vol. 29, No. 3, September 2014, pp. 602 – 610.

[90] T.K. Soon, S. Mekhilef: A Fast-Converging MPPT Technique for Photovoltaic System Under Fast-Varying Solar Irradiation and Load Resistance, IEEE Transactions on Industrial Informatics, Vol. 11, No. 1, February 2015, pp. 176 – 186.

[91] L.A. Zadeh: Fuzzy Sets, Information and Control, Vol. 8, No. 3, June 1965, pp. 338 – 353.

[92] L.- X. Wang: A Course in Fuzzy Systems and Control, Prentice Hall PTR, Upper Saddle River, NJ, 1997.

[93] O. Guenounou: Methodology for the design of intelligent controllers using the genetic approach: application to a bioprocess, Ph.D. Thesis, Université Toulouse III-Paul Sabatier, Toulouse, 2009. (In French).

[94] W. Pedrycz: Why Triangular Membership Functions?, Fuzzy Sets and Systems, Vol. 64, No. 1, May 1994, pp. 21 – 30.

[95] S. Karthika, K. Velayutham, P. Rathika, D. Devaraj: Fuzzy Logic Based Maximum Power Point Tracking Designed for 10kW Solar Photovoltaic System with Different Membership Functions, International Journal of Electrical and Computer Engineering, Vol. 8, No. 6, 2014, pp. 1022 – 1027.

[96] R. Eberhart, J. Kennedy: A New Optimizer Using Particle Swarm Theory, Proceedings of the 6th International Symposium on Micro Machine and Human Science (MHS'95), Nagoya, Japan, October 1995, pp. 39 – 43.

[97] Y. Cooren: Improvement of an adaptive Optimization algorithm by Particle Swarm: application in medical engineering and electronics, Ph.D. Thesis, Université de Paris, Paris, 2008. (In French).

[98] Z. Bingül, O. Karahan: A Fuzzy Logic Controller Tuned with PSO for 2 DOF Robot Trajectory Control, Expert Systems with Applications, Vol. 38, No. 1, January 2011, pp. 1017 – 1031.

[99] M. Clerc, J. Kennedy: The Particle Swarm – Explosion, Stability, and Convergence in a Multidimensional Complex Space, IEEE Transactions on Evolutionary Computation, Vol. 6, No. 1, February 2002, pp. 58 – 73.

[100] Z.- L. Gaing: A Particle Swarm Optimization Approach for Optimum Design of PID Controller in AVR System, IEEE Transactions on Energy Conversion, Vol. 19, No. 2, June 2004, pp. 384 – 391.

[101] A. Noshadi, J. Shi, W. S. Lee, P. Shi, A. Kalam: Optimal PID-Type Fuzzy Logic Controller for a Multi-Input Multi-Output Active Magnetic Bearing System, Neural Computing and Applications, Vol. 27, No. 7, October 2016, pp. 2031 – 2046.

[102] A. Jouda, F. Elyes, A. Rabhi, M. Abdelkader: Optimization of Scaling Factors of Fuzzy–MPPT Controller for Stand-Alone Photovoltaic System by Particle Swarm Optimization, Energy Procedia, Vol. 111, March 2017, pp. 954 – 963.

[103] J. Ahmed, Z. Salam: A Maximum Power Point Tracking (MPPT) for PV System Using Cuckoo Search with Partial Shading Capability, Applied Energy, Vol. 119, April 2014, pp. 118 – 130.

[104] N. Bouarroudj, D. Boukhetala, V. Feliu-Batlle, F. Boudjema, B. Benlahbib, B. Batoun: Maximum Power Point Tracker based on Fuzzy Adaptive Radial Basis Function Neural Network for PV-System, Energies, Vol. 12, No. 14, July 2019, 2827, pp. 1 – 19.